RAPID COMMUNICATIONS

PHYSICAL REVIEW B VOLUME 44, NUMBER 11 15 SEPTEMBER 1991-I

Metal-on-metal thin-film growth: Au/Ni(001) and Ni/Au(001)

W. D. Luedtke and Uzi Landman
School of Physics, Georgia Institute of Technology, Atlanta, Georgia 30332
(Received 8 March 1991; revised manuscript received 1 July 1991)

Growth modes and dynamics of vapor-deposited thin metal films on metal substrates are studied by means of molecular-dynamics simulations using embedded-atom interactions. Gold films deposited on a room-temperature Ni(001) substrate exhibit Stranski-Krastanov growth of Au(111) films, and growth of nickel films on Au(001) involves interspecies mixing and three-dimensional growth of strained films pseudomorphic to the substrate.

Recent advances in experimental epitaxial growth techniques greatly enhanced the capability to grow artificially structured materials.[1] While progress has been realized in theoretical descriptions[2–5] of the equilibrium thermodynamics and kinetics of growth, it is generally difficult to predict with these theories the growth mode and dynamics. In particular, at the initial thin-film stage some of the required quantities (such as interfacial energies) are poorly known, bulk values for material characteristic parameters (such as surface free energies) are not valid for systems in the few-monolayers-thickness regime, and, moreover, nonequilibrium conditions may dominate.

In this study we investigate by means of molecular-dynamics simulations,[6] employing realistic many-body embedded-atom-method (EAM) interaction potentials,[7] the dynamics and growth modes of thin metal films deposited on metal substrates. For the two metals, Au and Ni, which are immiscible in the bulk at room temperature (RT), we show that (i) deposition of gold on a Ni(001) substrate (at 300 K) results in a Au(111) film growing in a Stranski-Krastanov (SK) mode[8] [i.e., three-dimensional (3D) growth on top of an initially 2D grown monolayer]; (ii) deposition of nickel on Au(001) involves interspecies mixing leading to strained films pseudomorphic to the Au(001) substrate, which grow via a Volmer-Weber (VW) mode[9] (i.e., nucleation and growth of 3D clusters from the beginning of the process).

The simulated systems consisted of a substrate of five layers exposing a (001) surface with $n_l = 200$ atoms/layer which evolve dynamically subject to the EAM interactions,[7(b)] and are situated on top of two static layers of the same crystallographic orientation with a lattice spacing of the substrate material at 300 K. The system is then periodically repeated in the two directions parallel to the (001) surface (x,y). The kinetic temperature of the substrate is controlled to the desired temperature via scaling of particle velocity in the dynamic layer adjacent to the static substrate, and the equations of motion were integrated using Gear's fifth-order predictor-connector algorithm, with a time step $\Delta t = 3.05 \times 10^{-15}$ s.

Subsequent to equilibration of the substrate to the desired temperature, deposition occurs by releasing (at intervals of 10^3 Δt) particles normal to the surface from random positions on a (x,y) plane located outside the range of interaction above the surface, with an initial kinetic energy $E_k^0 = (3/2)k_B T_m$, where T_m is the melting temperature of the deposited material.

Prior to discussing results for film growth we remark on simulations[10] in which a single atom is released toward a clean equilibrated (300 K) substrate with E_k^0 as mentioned before, and the process repeated, for statistical purposes, starting from different initial conditions. From these simulations we conclude that both for Au atoms impinging on Ni(001), and for Ni atoms on Au(001), spatial and energetic accommodations occur rapidly; the potential and kinetic energies of the system achieve equilibrium values in 2–5 ps, with the major part of the energy exchange with the substrate occurring in less than 2 ps. The average distance traveled by an impinging atom parallel to the surface (measured from the point of initial interaction) is ~ 4.5 Å for a Ni atom impinging on Au(001) and ~ 1.6 Å for an Au atom on Ni(001) for normal incidence, and somewhat larger values for incidence of 60° from the surface normal (azimuthally averaged). These results guided our choice of deposition rate to optimize quasiequilibrium conditions.

Results for growth of Au films deposited on RT Ni(001) are shown in Fig. 1. The layer occupancies Θ_l [i.e., the number of atoms in layer l, normalized by the number of sites in the (001) substrate, i.e., $n_l = 200$] plotted in Fig. 1(a) versus the overall number of deposited atoms Θ_d (normalized by n_l), demonstrate clearly (see also Fig. 2) a characteristic SK growth mode, i.e., the onset of the second film layer, Θ_2, occurs after the first layer, Θ_1, is completely formed, and subsequent growth occurs via nucleation and coalescence of 3D islands. [Note that for a complete (111) layer adsorbed on the (001) substrate $\Theta_l = 0.9$.]

The structure of the deposited Au film is (111), rotated with respect to the Ni(001) substrate, and is driven by the large lattice mismatch between the two materials [a(Au)/a(Ni) $\sim 16\%$]. A plot of $f_{6,l}$, the fraction of sixfold-coordinated atoms in layer l vs Θ_d, shown in Fig. 1(b), reveals that the onset of the (111) structure in the first 2D layer ($l = 1$), occurs at $\Theta_d \sim 0.3$ and evolves rapidly thereafter. Further deposited layers exhibit (111) structure from the initial stages of their deposition.

Growth of the Au films has an indiscernable effect on the layer spacing in the Ni substrate (i.e., the distance at room temperature between the topmost Ni layer and the one underneath it is ~ 1.78 Å for both the bare and gold-covered substrate). The interlayer distances $d_{l,l-1}$ be-

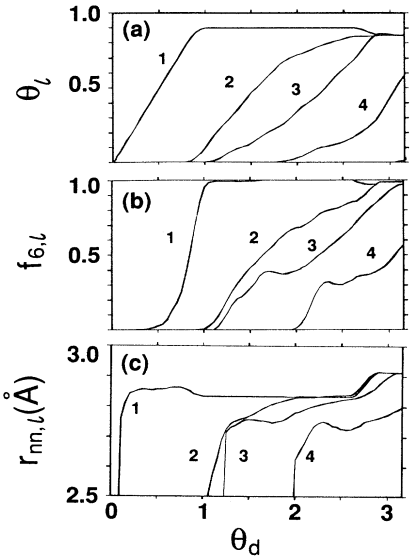

FIG. 1. Normalized layer occupancies Θ_l, the fraction of sixfold-coordinated atoms $f_{6,l}$, and the average interatomic nearest-neighbor distances in layers $r_{NN,l}$, plotted vs Θ_d (the total number of deposited atoms normalized by $n_l=200$) for deposition of a Au film on a 300-K Ni(001) substrate.

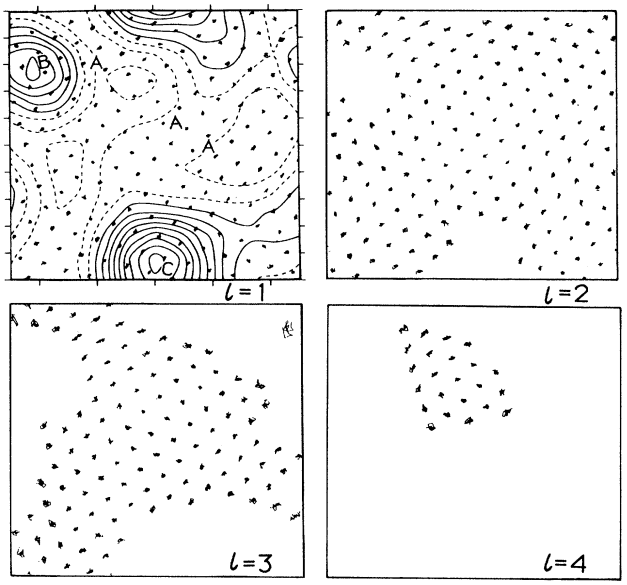

FIG. 2. Short-time trajectories of Au atoms in layers $l=1$–4, deposited on a 300-K Ni(001) substrate. Note the (111) structure of the film and the 3D nature of the growth mode. Superimposed on the structure of the first grown layer ($l=1$) are strain contours (ϵ). Solid and dashed lines correspond to positive and negative ϵ values, respectively (A, B, and C correspond to $\epsilon=0.17$, -0.5, and -1.0, respectively). The dimensions along the x,y direction are 35.2 Å.

tween layers l and $l-1$ of the Au film (with $l=1$ denoting the first Au layer and $l=0$ the topmost Ni surface layer) are $d_{1,0}=2.13$ Å, $d_{2,1}=2.43$ Å, $d_{3,2}=2.34$ Å compared to $d_{111}(\mathrm{Au})=2.36$ Å in bulk Au.

The structural evolution of the film is further illustrated in Fig. 1(c), where the average distances between nearest-neighbor atoms in layers l ($r_{NN,l}$) are shown versus Θ_d. An interesting structural transition is observed at $\Theta_d \gtrsim 2.5$, reflected also in Fig. 1(a) and characterized by a decrease in the occupancy of the first deposited Au(111) film, accompanied by an expansion of the intralayer interatomic distance. The structure of the system at the onset of the transformation is displayed in Figs. 2(a)–2(d), which also illustrates the three-dimensional nature of the growth at this stage. Furthermore, the strain contours [i.e., $\epsilon=100(d_{NN,1}-\bar{d}_{NN,1})/\bar{d}_{NN,1}$ where $\bar{d}_{NN,1}=2.83$ Å is the average nearest-neighbor distance] in the first Au layer exhibit a nonuniform distribution with $d_{NN,1}$ in the region covered by the incomplete second layer (dashed contours) larger than that in the exposed regions (solid contours). The two-dimensional pressure in the layer (calculated from the atomic stress tensors) is positive, indicating a tendency toward dilatation. The origin of the nonuniform strain distribution at this stage are the different embedding environments of atoms in the first Au layer. The transformation which follows is cooperative in nature and is achieved via expulsion of atoms from the first Au (and subsequently from the second layer to the third) accompanied by inlayer dilatation, and a decrease in the total potential energy of the system. (The 2D pressure in the layer decreases after the transformation but remains positive, indicating residual strain.)

It is interesting to remark that in simulations[11] of the adhesive interaction between a Au tip exposing a (001) facet and a 300-K Ni(001) substrate, we have observed a similar (111) reconstruction of the bottom region (~3–5 layers) of the tip. Furthermore, the number of reconstructed layers increases upon the development of tensile stress during separation of the two materials from the point of adhesive contact.

In contrast to the SK growth mode of a Au film on Ni(001), deposition of Ni atoms on a 300-K Au(001) substrate (as well as on a cold 100-K substrate) results in 3D growth starting from the initial stages of the growth process (i.e., VW mode) as may be seen from Fig. 3(b). Furthermore, the growth process involves atomic exchange and interspecies mixing as may be seen from the Au layer occupancies, Θ_l (Au), shown in Fig. 3(c), and the Au concentration profiles shown in Fig. 3(a) for both deposition conditions [300-K and 100-K Au(001) substrates]. As seen, the degree of interspecies mixing is larger for the film grown on the hotter substrate. In this context we remark that the tendency for an adsorbed Ni atom to exchange position with a neighboring Au atom located in the underlying layer is greatly enhanced when another Ni atom is adsorbed in a neighboring fourfold site.[10]

Finally, for the thin films which we have studied [see Figs. 3(a), 3(d), and 3(e)] the structure of the film is pseudomorphic to the Au(001) substrate, resulting in lateral strain in the layers, which in turn induces contraction of interlayer spacings ($d_{1,0}=1.61$ Å, $d_{2,1}=1.47$ Å, $d_{3,2}=1.41$ Å, and $d_{4,3}=1.35$ Å) in comparison to that between (001) layers in bulk Ni (1.76 Å). [The spacing between the topmost layer of the substrate and the next layer down is $d_{0,-1}=1.82$ Å, followed by $d_{-1,-2}=2.08$ Å,

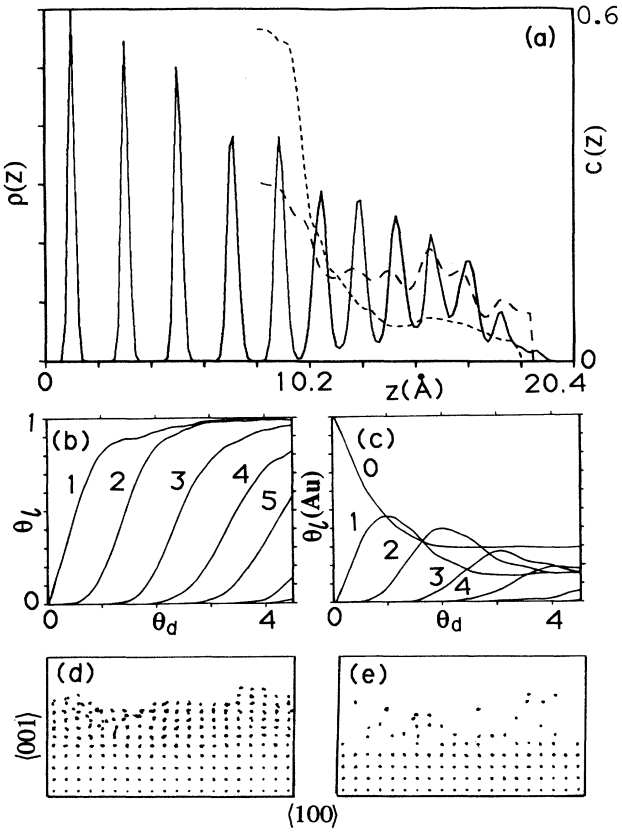

FIG. 3. Deposition of Ni on Au(001). (a) Particle number density $\rho(z)$, in arbitrary units, vs z (in Å). The original dynamic substrate consisted of five Au(001) layers starting from the left. The long- and short-dashed lines give the concentrations of Au atoms in the film (right-hand scale), for deposition on 300-K and 100-K Au(001) substrates, respectively. (b),(c) Normalized, total [in (b)] and gold [in (c)] occupancies vs Θ_d for deposition on a 300-K Au(001). (d),(e) 8-Å slices through the system viewed along the ⟨010⟩ direction. The original Au(001) dynamic substrate consisted of five bottom layers. The structure in (d) includes both Au and Ni atoms, and that in (e) the Au atom contribution to (d). The dimensions along the horizontal (⟨010⟩) and vertical axes in (d) and (e) are 40.8 Å and 24.5 Å, respectively.

and $d_{-2,-3}=2.04$ Å, which is close to the spacing between (100) planes in bulk Au.] Underlying the interlayer relaxation in the film is the density dependence of the cohesion energy which is explicitly included in the embedding energy functional.[7] In this context we remark that a simulation where the (001) plane of the Ni(100) substrate has been strained to that of the Au(001) lattice spacing (i.e., increased by 16%) yielded an interlayer spacing of 1.34 Å, in agreement with the value found in the grown nickel film away from the underlying gold substrate (i.e., compare $d_{4,3}=1.35$ Å). Furthermore, using linear elasticity theory for a nickel crystal, biaxially strained in the (001) plane by 16%, with the elastic constants of the EAM model,[7(b)] results in a spacing of 1.40 Å between (001) layers; in close agreement with the results of our simulations.

A view of the system along the ⟨010⟩ direction, given in Fig. 3(d), illustrates the pseudomorphic structure of the grown film, and the 3D nature of the growth process. The intermixing of Au atoms in the system is illustrated in Fig. 3(e), in which the separate contribution of the gold atoms to the structure in Fig. 3(d) is shown. It is of interest to remark that the intermixing which we observe correlates with the interfacial wetting of Ni by Au discussed by us previously in the context of the interaction between a Ni tip with an Au surface.[11]

In summary, our molecular-dynamics studies predict SK and VW modes of thin-film growth for the systems Au/Ni(001) and Ni/Au(001), respectively, with the Au film in the first system exhibiting a (111) structure. For the latter one interspecies mixing and a pseudomorphic strained structure are found. Microscopic dynamical mechanisms of the growth processes and their physical origins, related to the nature of cohesion in metals and the lattice mismatch between the two materials, were revealed.

We thank W. F. Egelhoff, Jr. for useful discussions. Research supported by U.S. Department of Energy (DOE) Grant No. FG05-86ER45234. Computations were performed at the National Energy Research Supercomputer Center, Livermore, CA, through a grant by the U.S. DOE.

[1]See reviews in *Layered Structures—Heteroepitaxy, Superlattices, Strain and Metastability,* edited by B. W. Dodson *et al.*, MRS Symposia Proceedings No. 160 (Materials Research Society, Pittsburgh, 1990); *Layered Structures and Epitaxy,* edited by J. M. Gibson, G. C. Osborn, and R. M. Tromp, MRS Symposia Proceedings No. 56 (Materials Research Society, Pittsburgh, 1986); J. W. Matthews, *Epitaxial Growth* (Academic, New York, 1975), Vols. A and B; W. F. Egelhoff, Jr., CRC Crit. Rev. Solid State Mater. Sci. **16**, 213 (1990).

[2]R. Kern, G. Le Lay, and J. J. Metois, in *Current Topics in Materials Science,* edited by E. Kaldis (North-Holland, Amsterdam, 1979), p. 135.

[3]E. Bauer, Appl. Surf. Sci. **11/12**, 479 (1982), and references therein.

[4]M. H. Grabow and G. H. Gilmer, Surf. Sci. **194**, 333 (1988).

[5]J. H. Van der Merwe and W. A. Jesser, J. Appl. Phys. **64**, 4968 (1988).

[6]For earlier MD simulations, see, e.g., B. W. Dodson, Surf. Sci. **184**, 1 (1987); P. A. Taylor and B. W. Dodson, Phys. Rev. **36**, 1355 (1987); W. D. Luedtke and U. Landman, Phys. Rev. B **40**, 11 733 (1989), and references therein.

[7](a) S. M. Foiles, M. I. Baskes, and M. S. Daw, Phys. Rev. B **33**, 7983 (1986); (b) J. B. Adams, S. M. Foiles, and W. G. Wolfer, J. Mater. Res. Soc. **4**, 102 (1989).

[8]J. N. Stranski and L. Krastanov, Ber. Akad. Wiss. Wien. **146**, 797 (1938).

[9]M. Volmer and A. Weber, Z. Phys. Chem. **119**, 277 (1926).

[10]W. D. Luedtke and U. Landman (unpublished).

[11]U. Landman and W. D. Luedtke, J. Vac. Sci. Technol. B **9**, 414 (1991); see also U. Landman *et al.*, Science **248**, 454 (1990).